

Tailoring sustainable compounds using eggshell membrane as biobased epoxy catalyst

Janetty Jany Pereira Barros¹ , Nichollas Guimarães Jaques¹ , Ingridy Dayane dos Santos Silva¹ , Ananda Karoline Camelo de Albuquerque¹ , Amanda Meneses Araújo²  and Renate Maria Ramos Wellen^{1,2*} 

¹Unidade Acadêmica de Engenharia de Materiais, Universidade Federal de Campina Grande – UFCG, Campina Grande, PB, Brasil

²Departamento de Engenharia de Materiais, Universidade Federal da Paraíba – UFPB, João Pessoa, PB, Brasil

*janetty_b@hotmail.com

Abstract

In this work eggshell membrane was added as biobased curing catalyst to epoxy (DGEBA), for comparison purposes the synthetic catalyst DEH 35 data was reported, the curing of compounds was followed through differential scanning calorimetry (DSC) under dynamic conditions and their kinetics were modeled using Kissinger, Friedman, Friedman model based and Málek approaches. From evaluated E_A and $\ln A$ two steps of curing were verified, for the synthetic catalyst compound (S_5) E_A abruptly increased for the degree of conversion $\alpha > 0.7$ the opposite trend was observed for the eggshell membrane compound (M_{10}). It is supposed for S_5 E_A increases due to the competitive reactions leading to viscosity increase until reach the solid phase with decrease of the reactive groups availability, hampering the cross-linking, whereas for M_{10} E_A decreases at $\alpha > 0.7$, hence invalidating the Kissinger model which assumes constant E_A .

Keywords: curing, eggshell membrane, epoxy, kinetics.

How to cite: Barros, J. J. P., Jaques, N. G., Silva, I. D. S., Albuquerque, A. K. C., Araújo, A. M., & Wellen, R. M. R. (2022). Tailoring sustainable compounds using eggshell membrane as biobased epoxy catalyst. *Polímeros: Ciência e Tecnologia*, 32(3), e2022025. <https://doi.org/10.1590/0104-1428.20210088>

1. Introduction

Epoxy resins are thermosets and represent polymers whose properties are considered superior to the conventional ones, which provide them extensive applications, ranging from coatings, adhesives to composites for electronics, sporting goods, aerospace, for instance^[1,2]. Epoxies properties are achieved through the cross-linking reactions, which occur between epoxy resin and hardening agent, promoting the reticulated network.

In resins which high performance is needed such as higher operating temperatures and greater mechanical strength, anhydrides as hardeners are conventionally added. However, the reactivity between epoxy and anhydride is low, resulting in longer times and temperatures for the curing end^[3]; and as a result it may initiate the degradation processes, impairing the epoxy polymerization as well as its final properties, hence catalysts addition are commonly used to accelerate the cure making the process feasible^[4,5]. The reaction of epoxides with cyclic anhydrides as the case of this paper, initiated by Lewis bases, proceeds through a chain wise polymerization, which comprises initiation, propagation, and termination or chain transfer steps^[6].

Searching sustainable alternatives for epoxy curing, the eggshell membrane is a natural by-product, considered a waste with low commercial value, however it has great

potential to act as an catalyst, due to its biologically active compounds; chemically it has 90% protein, 2% glucose and 2% mineral phases^[7]. Currently the membrane is used as biodiesel^[8,9] and bio compounds catalyst^[10,11]. Its potential to act in the curing is linked to its constituents, since the carboxylic functional groups, amino acids and sulfur present in structural proteins may act as curing catalysts^[12].

Epoxy/eggshell biocomposites have already been produced with the purpose of mechanical and thermal properties optimization^[13-15]. Saeb et al.^[16] carried out a comparative study between the non-isothermal curing kinetics of epoxy/CaCO₃ and epoxy/eggshell. The curing kinetics was investigated using Friedman, Ozawa, Kissinger - Akahira - Sunose and Málek models. Ozawa and KAS showed better agreement with the experimental data in relation to the Málek and Friedman ones. Nevertheless, using membrane as a catalyst is still scarcely explored. Jaques et al.^[17] investigated the curing kinetics of epoxies adding eggshell (E) or membrane (M) as curing catalysts, it was applied Ozawa, Kissinger, Friedman isoconversional, Friedman model based and Málek to model the curing. The results showed that only the membrane presented potential application as cross-linking performer. Related to the kinetic models, Málek and Friedman presented the

best adjustments to describe the curing of synthetic and bio-based compounds.

Eggshell and eggshell membranes as potential enhancers for epoxy systems were previously investigated by our research group, the results showed that the membrane increased the curing rate, and may be used as a low-cost substitute for synthetic catalysts. Regarding the thermal properties, composites with natural catalysts showed less stability^[18]. Aware that the final properties of epoxies depend on their cross-linking process, and this process is influenced by the cross-linkers, the processing variables (time, temperature, pressure), and knowing the influence that using a natural catalyst may provide in the epoxy curing, it is essential to investigate their curing kinetics.

Applying mathematical models to evaluate the curing kinetics helps to quantify the degree of conversion of epoxy compounds, in addition to providing reliable information such as identification of the curing mechanism, the activation energy (E_A), collision rate among molecules ($\ln A$). Additionally, from the comparison between theoretical and experimental data it is affordable to estimate the predictive power of the employed model, and afterwards its application in an industrial scale. Isoconversional models afford E_A variable along with the curing progress whereas the conventional ones assume it constant^[19-21].

Based on the above mentioned, this work aimed elucidating the curing kinetics of epoxy compounds (DGEBA)/eggshell membrane. The topic assumes great importance at both technological and scientific aspects since seldom works are focused on the membrane's abilities into thermosetting compounds, as further presented a costless crosslinker. Additionally, the kinetics investigation was conducted using differential scanning calorimeter (DSC) under dynamic conditions and the curing modeling was performed applying Kissinger, Friedman, Friedman model based and Málek models which parameters may be used as control tools to reach the desired conversion for specific property and application.

2. Materials and Methods

2.1 Materials

Diglycidyl ether of bisphenol A (DER 383) with epoxide equivalent weight of 176–186 g/eq, anhydride methyl tetrahydrophthalic (MTHPA) and 2,4,6-tris(dimethylaminomethyl) phenol (DEH 35) were supplied by Olin Corporation (São Paulo, Brazil). Chicken eggshell was supplied by a local farm (Campina Grande-PB, Brazil).

2.2 Eggshell membrane processing

Processing of membrane (M) was performed as an adapted methodology elsewhere proposed^[22]. Eggshell was washed in sodium hypochlorite (NaClO) and afterwards immersed in water for 2 h to remove the membrane. M was oven dried at 100 °C for 24 h. Afterwards, M was ground in a coffee mill B55 Botini (Bilac, SP, Brazil) and sieved through #200 mesh.

2.2.1 Compounding

Epoxy compounding at 100:87 (DER 383/MTHPA - resin/hardener) with DEH 35 at concentrations 0 and 5 phr (parts per hundred) were mixed in a magnetic stirrer for 5 min at 800 rpm.

M in content of 10 phr was added into 100:87 (DER 383/MTHPA). Afterwards, these compounds were mixed in a magnetic stirrer from Corning (Reynosa, Mexico) for 5 min at 800 rpm at ambient temperature (~23 °C). Compounds produced in this work are coded as presented in Table 1.

2.2.2 DSC measurements

The curing was followed up through differential scanning calorimetry (DSC) using a DSC Q20 from TA Instruments (New Castle, DE, USA). Samples of approximately 5 mg were tested in a standard closed aluminum pan, under a nitrogen gas flow of 50 mL/min. The samples were heated from 30 °C to 400 °C, at heating rates of 1, 2, 5, 10, and 20 °C/min. The theoretical background with the curing kinetics modeling information is presented in the Supplementary Material.

3. Results and Discussions

Figure 1 shows the DSC scans as time and temperature function for S_0 , S_5 and M_{10} for the applied heating rates. During heating, an exothermic peak characteristic of the epoxy curing is observed. For S_0 , Figure 1a, at heating rates higher than 2 °C/min, the exothermic peak is verified on the half-way due to unfinished curing. Reports mention that the curing of DGEBA/Anhydride without catalysts takes place together with degradation reactions, usually at temperatures above 300 °C^[5,23].

Additionally, to afore mentioned for the heating rates 5, 10 and 20 °C/min an endothermic peak is observed previously to the curing one (exothermic peak), which may be associated with the hardener (MTHPA) decomposition which starts at $T_i = 120$ °C and finishes at $T_f = 275$ °C, assuming nitrogen atmosphere and 10 °C/min as the heating rate, as reported elsewhere^[18]. For S_5 (synthetic catalyst added), Figure 1b, the curing presented a bell shape without discontinuities, indicating that for this system the reaction occurs through one mechanism, despite presenting lower time and temperature curing ranges^[24-26].

Upon eggshell membrane addition as the catalyst, the epoxy curing proceeded at intermediate times and temperatures related to S_0 and S_5 , Figure 1c-1d. Quantitatively in M_{10} , there

Table 1. Epoxy compounds and their component contents.

*Compositions	Epoxy Resin	Hardener	Catalyst	
	DER 383	MTHPA	DEH 35	Membrane
S_0	100	87	0	0
S_5	100	87	5	0
M_{10}	100	87	0	10

*S: synthetic compounds; M: compounds with eggshell membrane powder.

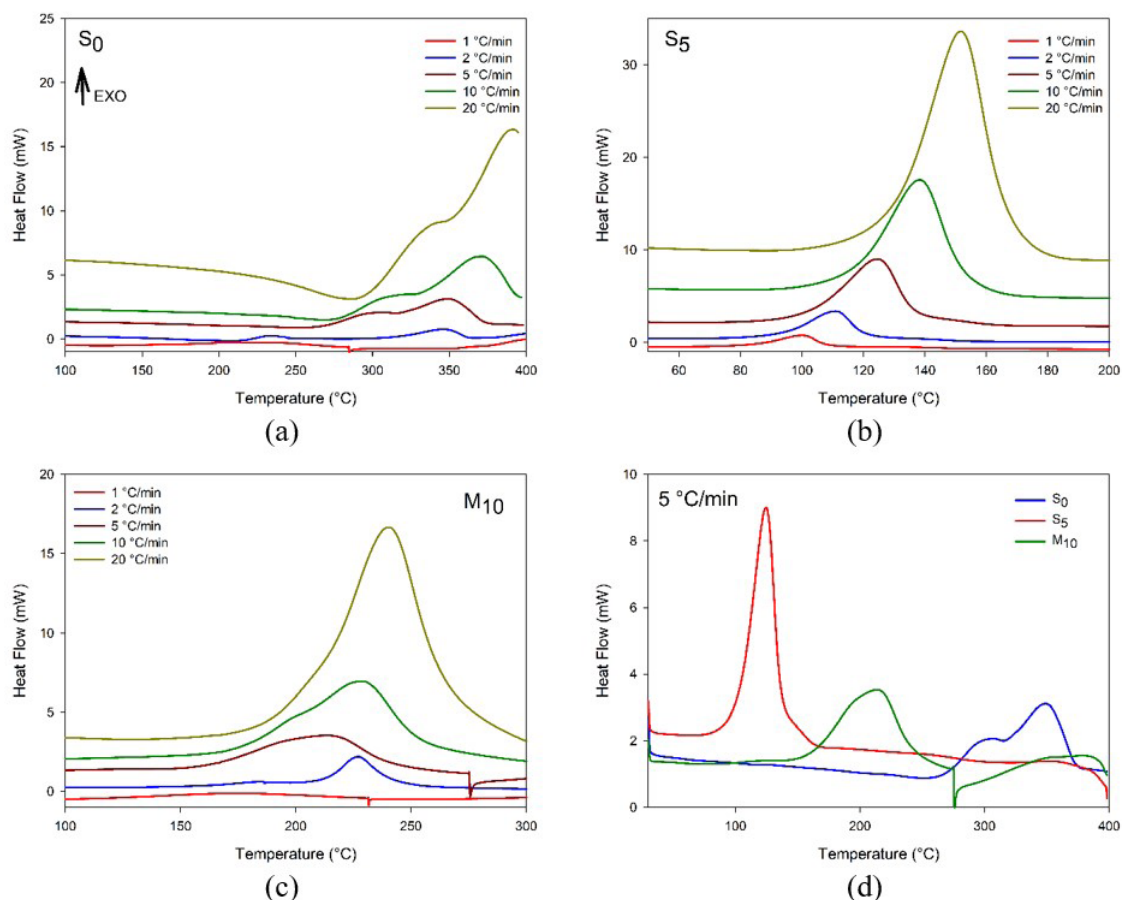


Figure 1. DSC scans of (a) S_0 ; (b) S_5 ; (c) M_{10} ; and (d) All compositions. Heating rates indicated.

is an increase of $65\text{ }^\circ\text{C}$ of $T_{0.01}$ related to S_5 for the heating rate $10\text{ }^\circ\text{C}/\text{min}$ (please see Table S1 of the Supplementary Material). Nevertheless, it is worth of mention adding the eggshell membrane the epoxy curing develops completely, occurs below $300\text{ }^\circ\text{C}$, and no degradation phenomena due to the MTHPA decomposition are verified. Therefore, may be assumed that the eggshell membrane properly acted as epoxy catalyst, as well as suggested that the curing initiation occurs through the amines and carboxyl present in the membrane proteins, as illustrated in Figure 2^[17].

Figure 3a shows the relative degree of conversion as temperature function and Figure 3b the conversion rate as the degree of conversion function for S_5 and M_{10} compositions.

Figure 3a illustrates epoxy compounds' sigmoid as verified discontinuities are absent indicating that a sole process took place, this trend is typical of DGEBA curing under non-isothermal conditions, it may be suggested the curing occurred through the autocatalytic mechanism.

In general, the acquired sigmoid may be analyzed into three stages:

- In the first stage, $0 \leq \alpha \leq 5\%$, the curing rate is slow and gradually increases. In this stage the curing initiation through catalysis and formation of the first active centers take place, for the epoxy compounds produced in the

present work these phenomena may proceed by two mechanisms:

- Esterification between the anhydride and the epoxy, whereas initially, the anhydride reacts with the epoxy's hydroxyls and afterwards the produced carboxyl reacts with the epoxide ring. In S_0 these processes would occur without initiator thus at longer times;
 - Anhydride activation through the synthetic (DEH 35) or natural (membrane) initiator, followed by the oxirane ring opening.
- In the second stage, $5 \leq \alpha \leq 90\%$, the curing rate increases due to the reactive functional groups availability and easier molecular movement;
 - In the third stage, $90 \leq \alpha \leq 100\%$, the curing rate decreases due to the lower functional groups availability together with the viscosity increase resulted from the cross-linking^[25-28].

Comparing Figure 3a-3b it may be observed that for S_5 the curing proceeded at lower temperatures and higher rates than M_{10} , which is resulted from the higher reactivity of synthetic catalyst (DEH 35). Nevertheless the membrane

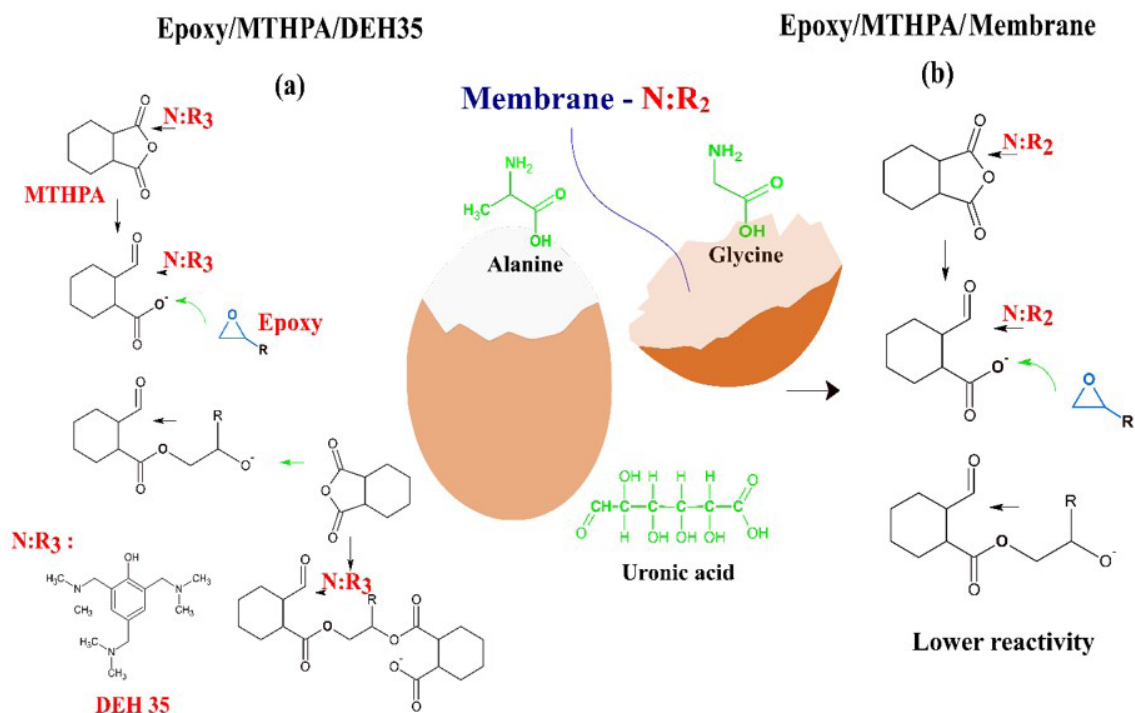


Figure 2. Proposed reactions. (a) Oxirane ring opening by DEH35; (b) Oxirane ring opening by the eggshell membrane.

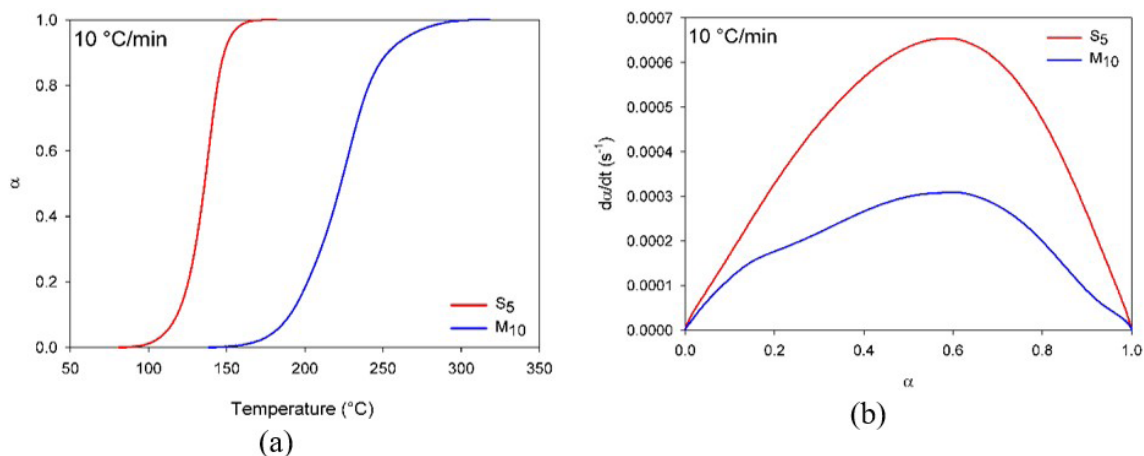


Figure 3. Degree of conversion (a); and Conversion rate (b) as temperature function. Heating rate 10 °C/min.

also promoted the curing through its main constituents such as glycine, alanine and uronic acid, once the amine and carbonyl groups in these constituents are potential catalysts^[12,29]; the catalysis process occurs similarly to the synthetic one but slower. Figure 2 illustrates the proposed scheme for the epoxy curing under addition of synthetic (S_5) and natural (M_{10}) catalysts. The amino acid molecules attack the anhydride. Nevertheless, it must be considered that both the secondary amine and the hydroxyl group can also react with the oxirane ring.

Both curing reagents and process variables are the key controllers, aiming to understand and define the rational parameters the kinetic modeling is indispensable as bellow discussed.

3.1 Kissinger's model

Plots in Figure 4 compare the experimental and theoretical degree of conversion as temperature function, and Figure S4 displays the discrepancy between these data estimated using the Kissinger model, which did not result in proper fits, being more evident for $0 \leq \alpha \leq 0.5$ with

discrepancies higher than 10% for S_5 ; whereas for M_{10} it was approximately 17% at 2 °C/min.

The Kissinger model estimates the global activation energy evaluated from the slope of linear regression $\ln(\beta/T_p^2)$ versus $1000/T_p$ (see Supplementary Material, Figure S9). However, it is feasible to consider E_A as variable and increasing along with the curing, because upon higher α the reagents content and the active centers decrease, while the viscosity increases, translating in higher energy expenses to promote the curing.

Additionally, in Kissinger model T_p is adopted to calculate the kinetics parameters; however E_A in T_p very likely differs between the initial and final stages^[30]. It is believed, E_A is function not only of temperature, but also of α , thus contributing to the discrepancy above verified and explaining the Kissinger inadequacy^[26,27,31,32].

Alternatively, the Friedman Isoconversional model was applied aiming to evaluate E_A along with α .

3.2 Friedman's isoconversional model

Figure 5 displays the plots of E_A and $\ln A$ as (α) function. Analyzing E_A in the range $\alpha > 0.7$, S_5 and M_{10} presented distinct trends while for S_5 E_A abruptly increases the reverse occurs with M_{10} , the same trend is verified for $\ln A$.

It is suggested for S_5 in the range $\alpha > 0.7$ E_A increases due to the competitive reactions leading to viscosity increase until reach the solid phase with decrease of the reactive groups availability, hampering the cross-linking.

Since, curing is followed by physical change of reaction medium. Initially, medium is a liquid composed of comonomers and newly formed oligomers. As the reaction progress, the oligomer/polymer's molecular weight increases, as does the viscosity and glass transition temperature. Molecular mobility decreases. The most dramatic decrease in mobility is associated to the polymer chains crosslinking, whereas the medium changes from flowing liquid to solid that can be rubbery or glassy (gelling and vitrification). Cross-linked

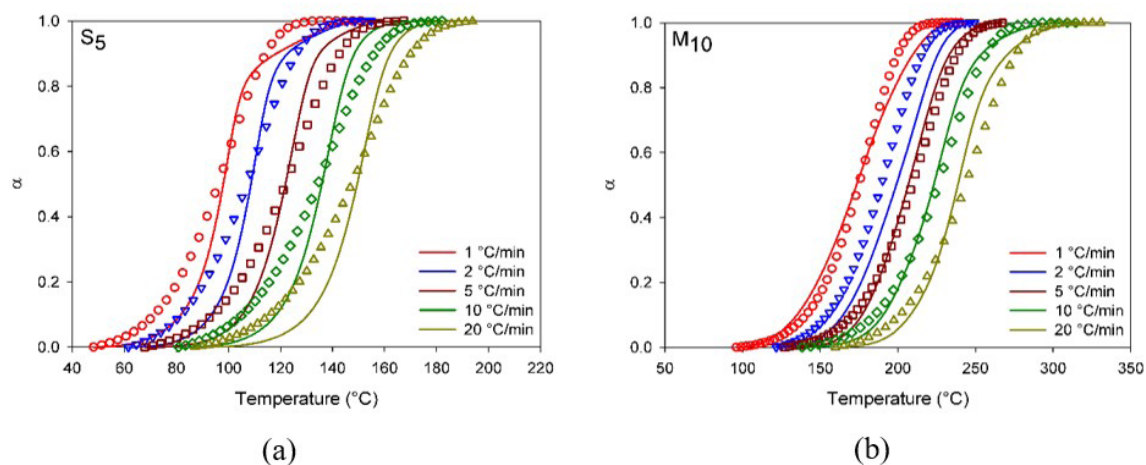


Figure 4. Comparison between the experimental (lines) and theoretical (symbols) α , estimated using Kissinger model at indicated rates. (a) S_5 ; and (b) M_{10} .

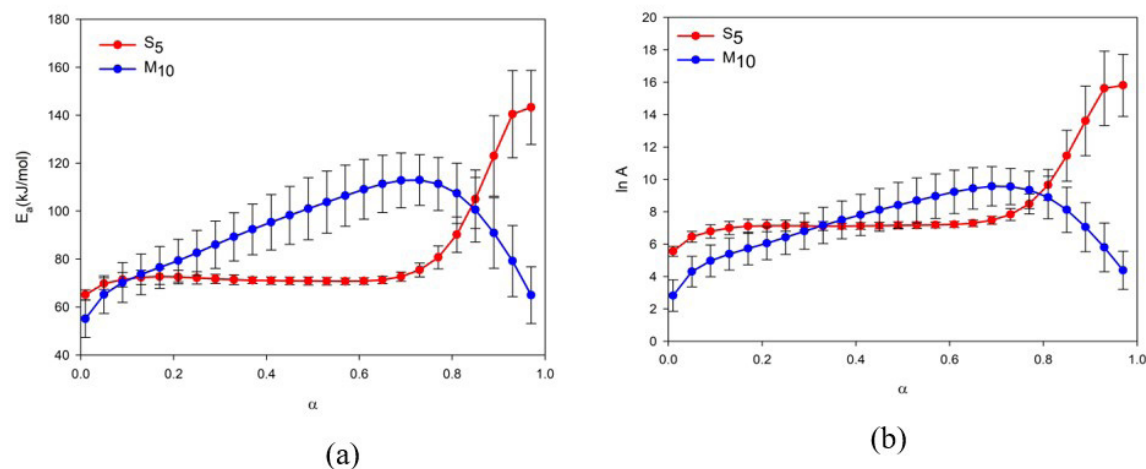


Figure 5. Kinetics parameters of Friedman Isoconversional Model. (a) E_A versus α ; and (b) $\ln A$ versus α .

chains lose the ability to move over each other, providing greater molecular collision as seen in $\ln A$ ^[25-27,33]. Formation of glassy solid (i.e., vitrification) occurs when the glass transition temperature rises above the actual curing temperature. In both cases, dramatic decrease in molecular mobility affects the curing kinetics which becomes controlled by the reagents diffusion. This curing complexity leads to complex kinetic behavior that can be detected in E_a changes with the curing progress. Free volume allowing only local movements of chain segments providing an increase in the overall E_a ^[33-37].

For M_{10} E_a increases in the range $0.1 < \alpha < 0.7$ due to reticulations processes as above mentioned. Nevertheless, for the range $\alpha > 0.7$ it decreases, from literature database it is suggested, this fact implied the rate-determining step of the reaction generally changed from the reaction control to the diffusion limitation. The reason lied in that molecular chains mobility of reactive species became more limited due to the increased junction points and gradually elevated glass temperature, which greatly restricted configuration rearrangements and cooperative motions of the network chains, especially as the reaction system approached its glassy state^[34,38].

Figure 6 illustrates the theoretical and experimental plots of α as temperature function for S_5 and M_{10} , and Figure S5 (Supplementary Material) its discrepancies. Reasonable fits were gathered for both compounds with mean errors lower than 5%, exception is valid for M_{10} at 2 °C/min with deviation 13% that does not disqualify the model.

3.3 Friedman's model based

Investigation of the curing mechanisms was also performed through the linear regression of $\ln[Af(\alpha)]$ versus $\ln(1-\alpha)$, Equation 9, these plots are displayed in Figure 7. S_5 and M_{10} presented an inflexion point on the conversion range of 0.4 and 0.23, respectively, this profile suggests compounds have similar curing mechanism, i.e., autocatalytic^[16,24,25]. According to the literature, the autocatalytic mechanism best describes the curing of epoxy/anhydride due to OH formation that catalyzes the curing; these reactive functional

groups are generated by esterification, corroborating the sigmoid profiles as shown in Figure 4^[39-41].

Aiming to effectively confirming the autocatalytic mechanism through the curing of S_5 e M_{10} the kinetics parameters E_a , $\ln A$ and n were evaluated from the linear and angular coefficients of $\ln[Af(\alpha)]$ versus $\ln(1-\alpha)$, (linear zone) which range from -6 to 0.4. Based on these parameters theoretical plots were built for the autocatalytic Friedman model which are compared with the experimental ones in Figure 8 and their discrepancy is showed in Figure S6. Plots presented quite reasonable fits with errors lower than 10%, exception is valid for S_5 and M_{10} at 1 °C/min with errors of 12% and 23%, respectively, due to higher deviation as verified at lower heating rates.

3.4 Malek's model

The functions of the Málek model $y(\alpha)$ and $Z(\alpha)$ as well as their maximum α_m and α_p were measured for S_5 and M_{10} at the rate 20°C/min and are illustrated in Figure 9, (the other data are presented in Supplementary Material) both plots presented concave profile and agree with the criterion $0 < \alpha_m < \alpha_p \neq 0.632$, indicating the curing is autocatalytic, as previously verified by autocatalytic Friedman model.

From the parameter α_m the linear regression $\ln\left[\frac{da}{dt} \cdot e^{(E_a/RT)}\right]$ versus $\ln[a^p(1-a)]$, Equation 14 was plotted afterwards the kinetics parameters $\ln A$ and $n+m$ were estimated and are presented in Figure 10. As well as the autocatalytic Friedman linear regression the Málek regression displayed a roll with an inflection point indicating that the curing of S_5 and M_{10} follows the autocatalytic mechanism, corroborating results already presented in Figure 9. Additionally, linear deviation was verified for the heating rates 1 °C/min and 2 °C/min, as also observed for the autocatalytic Friedman model.

As Málek model is unable to provide E_a the average E_a evaluated based on the isoconversional Friedman model was applied to determine the kinetics parameters $\ln A$, n and m through Equation 14. Afterwards, theoretical plots

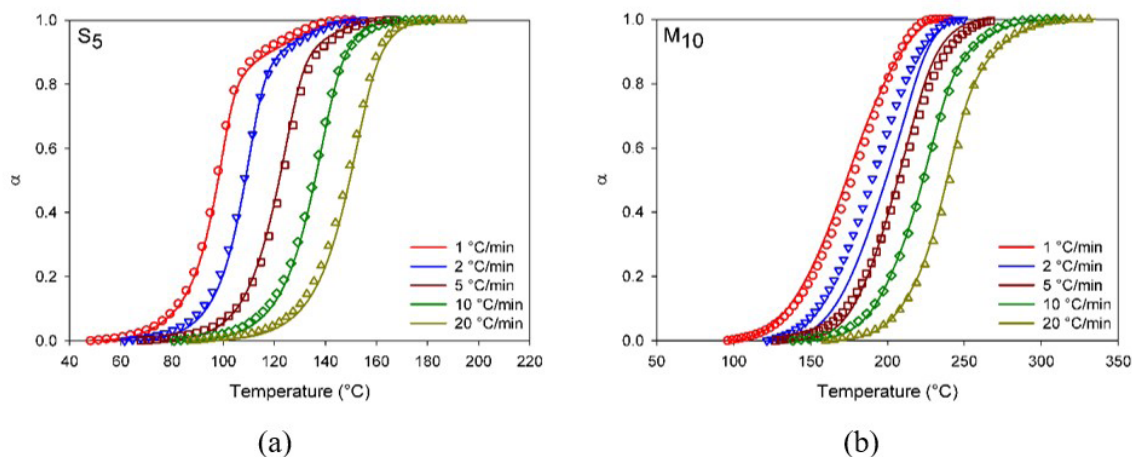


Figure 6. Comparison between theoretical (symbol) and experimental (lines) α computed using the Friedman Isoconversional model at indicated heating rates. (a) S_5 ; and (b) M_{10} .

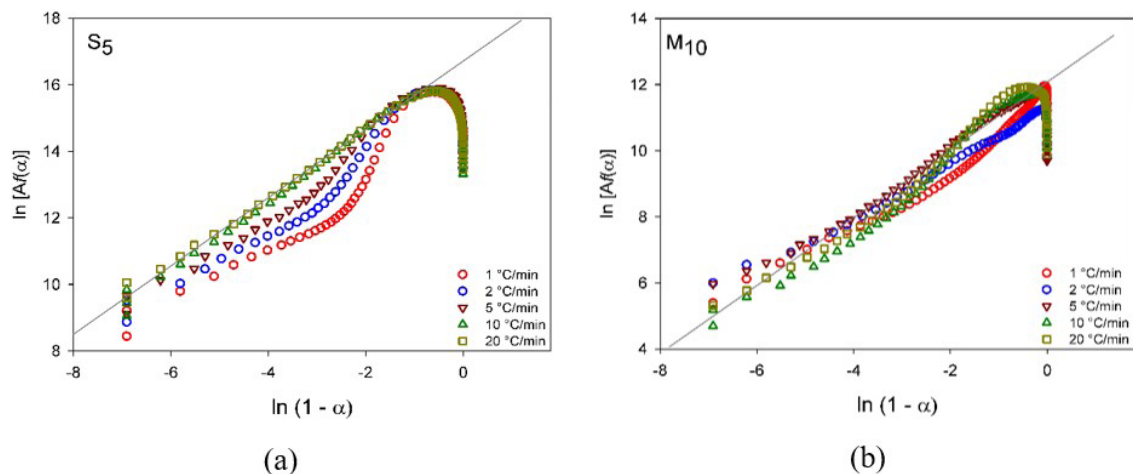


Figure 7. Linear regression of Friedman $\ln[Af(\alpha)]$ versus $\ln(1-\alpha)$, Equation 9. (a) S_5 ; and (b) M_{10} .

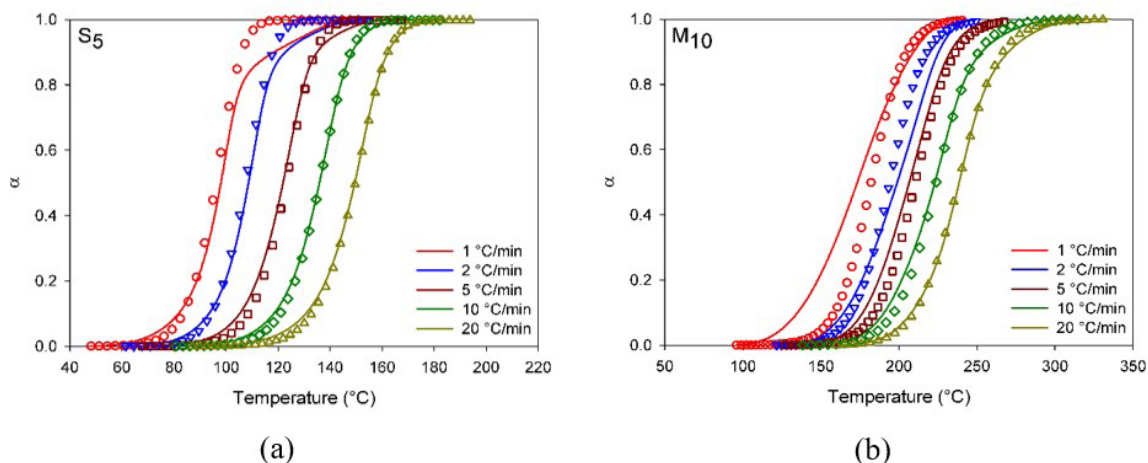


Figure 8. Experimental (lines) and theoretical (symbols) α evaluated using the autocatalytic Friedman model at the indicated heating rates. (a) S_5 ; and (b) M_{10} .

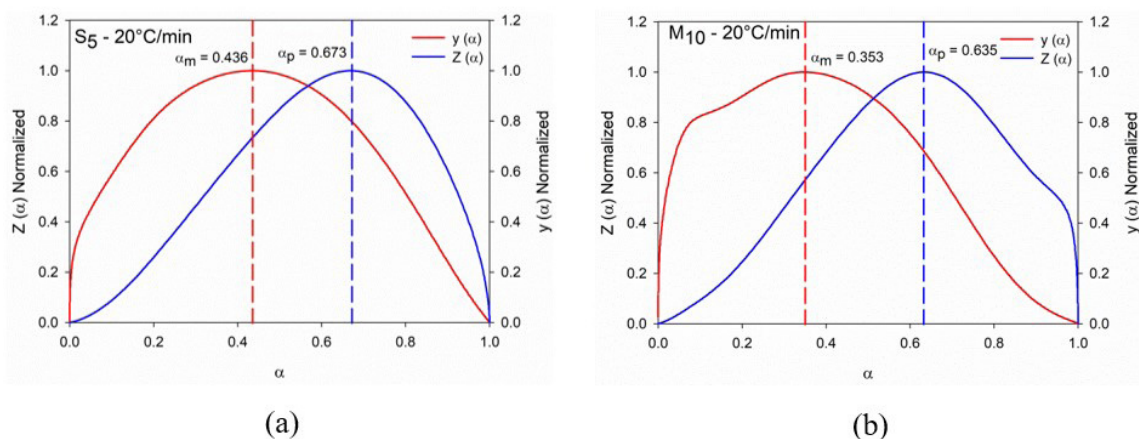


Figure 9. Málek functions $y(\alpha)$ and $Z(\alpha)$ computed at 20 °C/min. (a) S_5 ; and (b) M_{10} .

were built compared with the experimental ones as shown in Figure 11, their deviations are displayed in Figure S7. From Figure 11 proper correlation is verified for the Málek model in all applied heating rates for S₅ and M₁₀, which is corroborated by a maximum error of approximately 12%.

3.5 Comparative

The kinetic parameters E_A , $\ln A$ and $n+m$ evaluated using the applied models in this work for S₅ and M₁₀ are shown in Table 2. Summing up E_A displays distinct profile for S₅ and M₁₀ with a maximum difference of 29.85 kJ/mol through Friedman model based on the autocatalytic mechanism. Related to $\ln A$, with exception of autocatalytic Friedman model, S₅ resulted in higher values with maximum difference of 4.9 for Málek model when compared to M₁₀, which suggests in S₅ there are much molecular collision. These results indicate the curing reaction is more favorable for S₅ than

for M₁₀, corroborating the results of Figure 1 and Figure 3, confirming the greater reactivity of the synthetic initiator.

Regarding the parameter $n+m$ for both compositions, it is higher than 1 confirming the complex curing profile and following the autocatalytic mechanism, which justifies E_A variation along with the whole reaction, as also discussed in Figure 5. Additionally, these results are on line with those previously reported for curing in epoxy/anhydride resins^[16,42].

In order to select the most appropriate model to describe the curing the theoretical and experimental plots of $d\alpha/dt$ are compared in Figure 12, and their discrepancies are in Figure S8. Applied models displayed proper fits with discrepancies lower than 5%, the exception was verified for Kissinger which was approximately 15%.

Isoconversion models by integration such as Kissinger are limited to determine E_a , since affords an overall E_a , which adds errors to the evaluation. However, it was observed for

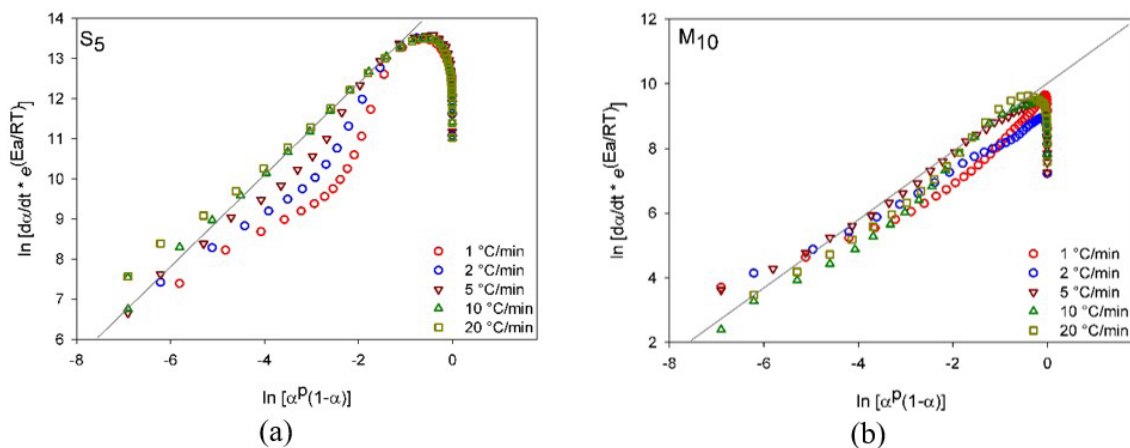


Figure 10. Linear regression of Málek $\ln \left[\frac{d\alpha}{dt} \cdot e^{\left(\frac{E_a}{RT} \right)} \right]$ versus $\ln \left[a^P (1-a) \right]$, Equation 13. (a) S₅; and (b) M₁₀.

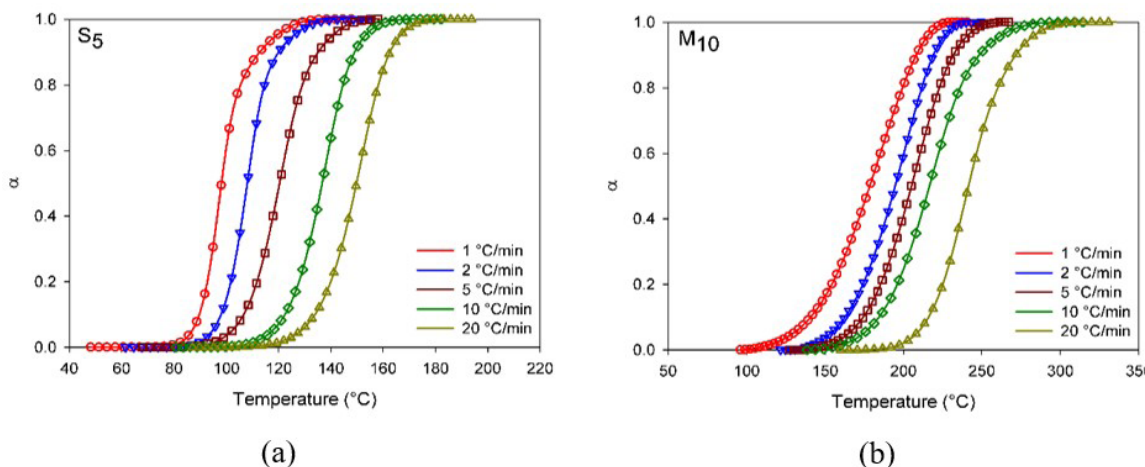
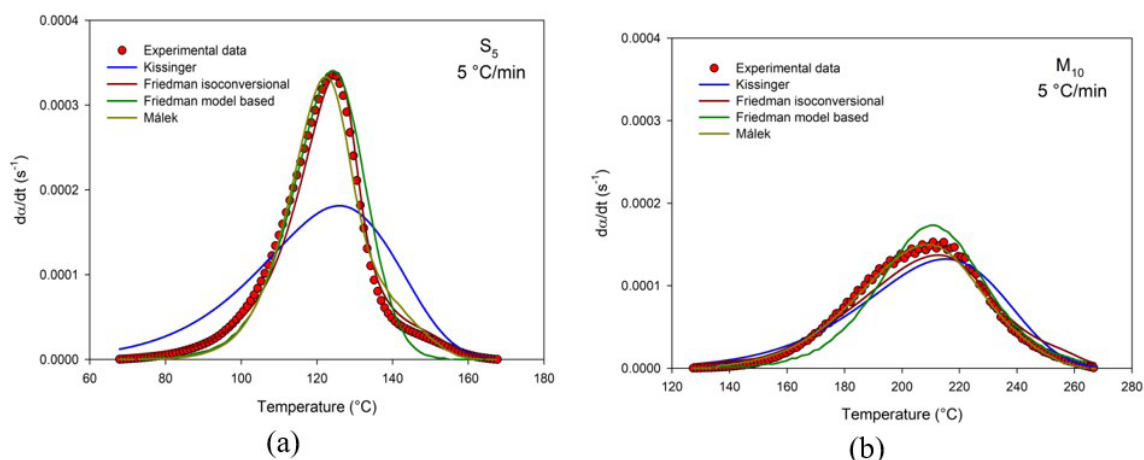


Figure 11. Comparison between experimental (lines) and theoretical (symbols) α estimated using Málek model at indicated heating rates. (a) S₅; and (b) M₁₀.

Table 2. Kinetics parameters of S_5 and M_{10} .

Compounds		Kissinger	Friedman Isoconversional	Friedman Model Based*	Málek
S_5	E_a (kJ/mol)	69.9 ± 1.1	77.0 ± 3.8 ¹	66.7	77.0 ± 3.8 ²
	$\ln A$ (ln (1/s))	15.6 ± 0.3	18.1 ± 0.3 ¹	15.7	15.0 ± 0.8
	$n+m$	-	-	1.6	3.0 ± 1.1
	R^2	0.8716	0.9955	0.9979	-
M_{10}	E_a (kJ/mol)	76.9 ± 20.3	96.6 ± 11.3 ¹	96.6	96.6 ± 11.3 ²
	$\ln A$ (ln (1/s))	13.2 ± 5.0	18.1 ± 2.8 ¹	18.9	10.1 ± 0.6
	$n+m$	-	-	1.8	1.1 ± 0.4
	R^2	0.9329	0.9937	0.9928	-

¹Average E_a and $\ln A$ based on Friedman Isoconversional model. ²Average E_a based on Friedman Isoconversional for Málek model. *Presented data are without error/uncertainty range once the used software does not provide them.

**Figure 12.** Comparison between experimental and theoretical $d\alpha/dt$ for applied models at the heating rate of 5 °C/min (a) S_5 ; and (b) M_{10} .

Friedman Isoconversional, as shown in Figure 5, for S_5 curing, E_a developed in two stages, in the almost constant followed by the second with an ascending profile at the curing end, such variation invalidates the curing assessment by Kissinger.

For M_{10} E_a also changed along with the curing, hence invalidating Kissinger model. Summing up, the isoconversional Friedman, Friedman model based and Málek models are suitable for describing the curing of S_5 and M_{10} resins.

4. Conclusion

Epoxy compounds with eggshell membrane and DEH 35 were kinetically investigated in this work and their parameters were evaluated using Kissinger, Friedman, Friedman model based and Málek models. From the DSC scans in M_{10} the curing occurs through one mechanism, despite presenting higher time and temperature related to S_5 . Nevertheless, it is worth of mention adding the eggshell membrane the epoxy curing develops completely as verified on DSC scans. Therefore, may be assumed that the eggshell membrane properly acted as epoxy curing catalyst. Applied models displayed proper fits with discrepancies lower than 5%, the exception was verified for Kissinger which

was approximately 15% most due to the activation energy changes along with the curing.

5. Author's Contribution

- **Conceptualization** – Janetty Jany Pereira Barros; Nichollas Guimarães Jaques.
- **Data curation** – Janetty Jany Pereira Barros; Nichollas Guimarães Jaques; Ingridy Dayane dos Santos Silva; Ananda Karoline Camelo de Albuquerque; Amanda Meneses Araújo.
- **Formal analysis** – Janetty Jany Pereira Barros; Nichollas Guimarães Jaques.
- **Investigation** – Janetty Jany Pereira Barros; Nichollas Guimarães Jaques.
- **Methodology** – Nichollas Guimarães Jaques; Renate Maria Ramos Wellen.
- **Project administration** – Renate Maria Ramos Wellen.
- **Resources** – Renate Maria Ramos Wellen.
- **Software** – Nichollas Guimarães Jaques; Janetty Jany Pereira Barros.
- **Supervision** – Renate Maria Ramos Wellen.

- **Validation** – Nichollas Guimarães Jaques; Janetty Jany Pereira Barros; Renate Maria Ramos Wellen.
- **Visualization** – Nichollas Guimarães Jaques; Janetty Jany Pereira Barros; Renate Maria Ramos Wellen.
- **Writing – original draft** – Janetty Jany Pereira Barros; Nichollas Guimarães Jaques; Ingridy Dayane dos Santos Silva; Renate Maria Ramos Wellen.
- **Writing – review & editing** – Janetty Jany Pereira Barros; Nichollas Guimarães Jaques; Renate Maria Ramos Wellen.

6. Acknowledgements

The authors would like to acknowledge the financial support from the Coordenação de Aperfeiçoamento de Pessoal de Nível Superior (CAPES), from Conselho Nacional de Desenvolvimento Científico e Tecnológico (CNPq) and Fundação de Apoio à Pesquisa do Estado da Paraíba (FAPESQ) (Concession term: 017/2019). Professor Renate Wellen is CNPq fellow (Number: 307488/2018-7). The authors would like to thank Olin Corporation (Brazil) for kindly supplying the reactants.

7. References

1. Qi, B., Zhang, Q. X., Bannister, M., & Mai, Y.-W. (2006). Investigation of the mechanical properties of DGEBA-based epoxy resin with nanoclay additives. *Composite Structures*, 75(1-4), 514-519. <http://dx.doi.org/10.1016/j.compstruct.2006.04.032>.
2. Tang, L., & Weder, C. (2010). Cellulose whisker/epoxy resin nanocomposites. *ACS Applied Materials & Interfaces*, 2(4), 1073-1080. <http://dx.doi.org/10.1021/am900830h>. PMID:20423128.
3. Uglea, C. V. (1998). *Oligomer technology and applications*. Boca Raton: CRC Press. <http://dx.doi.org/10.1201/9780585392233>.
4. Criado, J. M., Málek, J., & Ortega, A. (1989). Applicability of the master plots in kinetic analysis of non-isothermal data. *Thermochimica Acta*, 147(2), 377-385. [http://dx.doi.org/10.1016/0040-6031\(89\)85192-5](http://dx.doi.org/10.1016/0040-6031(89)85192-5).
5. Montserrat, S., Flaqué, C., Calafell, M., Andreu, G., & Málek, J. (1995). Influence of the accelerator concentration on the curing reaction of an epoxy-anhydride system. *Thermochimica Acta*, 269-270, 213-229. [http://dx.doi.org/10.1016/0040-6031\(95\)02362-3](http://dx.doi.org/10.1016/0040-6031(95)02362-3).
6. Pascault, J.-P., Sautereau, H., Verdu, J., & Williams, R. J. J. (2002). *Thermosetting polymers*. Boca Raton: CRC Press. <http://dx.doi.org/10.1201/9780203908402>.
7. Mine, Y. (2008). *Egg bioscience and biotechnology*. New York: John Wiley & Sons. <http://dx.doi.org/10.1002/9780470181249>.
8. Sharma, Y. C., Singh, B., & Korstad, J. (2010). A application of an efficient nonconventional heterogeneous catalyst for biodiesel synthesis from *Pongamia pinnata* Oil. *Energy & Fuels*, 24(5), 3223-3231. <http://dx.doi.org/10.1021/ef901514a>.
9. Wei, Z., Xu, C., & Li, B. (2009). Application of waste eggshell as low-cost solid catalyst for biodiesel production. *Bioresource Technology*, 100(11), 2883-2885. <http://dx.doi.org/10.1016/j.biortech.2008.12.039>. PMID:19201602.
10. Mosaddegh, E. (2013). Ultrasonic-assisted preparation of nano eggshell powder: a novel catalyst in green and high efficient synthesis of 2-aminochromenes. *Ultrasonics Sonochemistry*, 20(6), 1436-1441. <http://dx.doi.org/10.1016/j.ultsonch.2013.04.008>. PMID:23684545.
11. Laca, A., Laca, A., & Díaz, M. (2017). Eggshell waste as catalyst: a review. *Journal of Environmental Management*, 197, 351-359. <http://dx.doi.org/10.1016/j.jenvman.2017.03.088>. PMID:28407598.
12. Ji, G., Zhu, H., Qi, C., & Zeng, M. (2009). Mechanism of interactions of eggshell microparticles with epoxy resins. *Polymer Engineering and Science*, 49(7), 1383-1388. <http://dx.doi.org/10.1002/pen.21339>.
13. Xu, Z., Chu, Z., Yan, L., Chen, H., Jia, H., & Tang, W. (2019). Effect of chicken eggshell on the flame-retardant and smoke suppression properties of an epoxy-based traditional APP-PEL system. *Polymer Composites*, 40(7), 2712-2723. <http://dx.doi.org/10.1002/pc.25077>.
14. Hamdi, W. J., & Habubi, N. F. (2018). Preparation of epoxy chicken eggshell composite as thermal insulation. *Journal of the Australian Ceramic Society*, 54(2), 231-235. <http://dx.doi.org/10.1007/s41779-017-0145-4>.
15. Azman, N. A. N., Islam, M. R., Parimalam, M., Rashidi, N. M., & Mupit, M. (2020). Mechanical, structural, thermal and morphological properties of epoxy composites filled with chicken eggshell and inorganic CaCO₃ particles. *Polymer Bulletin*, 77(2), 805-821. <http://dx.doi.org/10.1007/s00289-019-02779-y>.
16. Saeb, M. R., Ghaffari, M., Rastin, H., Khonakdar, H. A., Simon, F., Najafi, F., Goodarzi, V., Vijayan, P. P., Puglia, D., Asl, F. H., & Formela, K. (2017). Biowaste chicken eggshell powder as a potential cure modifier for epoxy/anhydride systems: competitiveness with terpolymer-modified calcium carbonate at low loading levels. *RSC Advances*, 7(4), 2218-2230. <http://dx.doi.org/10.1039/C6RA24772E>.
17. Jaques, N. G., Souza, J. W. L., Popp, M., Kolbe, J., Fook, M. V. L., & Wellen, R. M. R. (2020). Kinetic investigation of eggshell powders as biobased epoxy catalyzer. *Composites. Part B, Engineering*, 183, 107651. <http://dx.doi.org/10.1016/j.compositesb.2019.107651>.
18. Jaques, N. G., Barros, J. J. P., Silva, I. D. S., Popp, M., Kolbe, J., & Wellen, R. M. R. (2020). New approaches of curing and degradation on epoxy/eggshell composites. *Composites. Part B, Engineering*, 196, 108125. <http://dx.doi.org/10.1016/j.compositesb.2020.108125>.
19. Vyazovkin, S. (2017). Isoconversional kinetics of polymers: the decade past. *Macromolecular Rapid Communications*, 38(3), 1600615. <http://dx.doi.org/10.1002/marc.201600615>. PMID:28009078.
20. Vyazovkin, S. (1997). Evaluation of activation energy of thermally stimulated solid-state reactions under arbitrary variation of temperature. *Journal of Computational Chemistry*, 18(3), 393-402. [http://dx.doi.org/10.1002/\(SICI\)1096-987X\(199702\)18:3<393::AID-JCC9>3.0.CO;2-P](http://dx.doi.org/10.1002/(SICI)1096-987X(199702)18:3<393::AID-JCC9>3.0.CO;2-P).
21. Ton-That, M.-T., Ngo, T.-D., Ding, P., Fang, G., Cole, K. C., & Hoa, S. V. (2004). Epoxy nanocomposites: analysis and kinetics of cure. *Polymer Engineering and Science*, 44(6), 1132-1141. <http://dx.doi.org/10.1002/pen.20106>.
22. Souza, J. W. L., Jaques, N. G., Popp, M., Kolbe, J., Fook, M. V. L., & Wellen, R. M. R. (2019). Optimization of epoxy resin: an investigation of eggshell as a synergic filler. *Materials*, 12(9), 1489. <http://dx.doi.org/10.3390/ma12091489>. PMID:31071924.
23. Galy, J., Sabra, A., & Pascault, J.-P. (1986). Characterization of epoxy thermosetting systems by differential scanning calorimetry. *Polymer Engineering and Science*, 26(21), 1514-1523. <http://dx.doi.org/10.1002/pen.760262108>.
24. Shanmugaraj, A. M., & Ryu, S. H. (2012). Study on the effect of aminosilane functionalized nanoclay on the curing kinetics of epoxy nanocomposites. *Thermochimica Acta*, 546, 16-23. <http://dx.doi.org/10.1016/j.tca.2012.07.026>.
25. Nonahal, M., Rastin, H., Saeb, M. R., Sari, M. G., Moghadam, M. H., Zarrintaj, P., & Ramezanzadeh, B. (2018). Epoxy/PAMAM dendrimer-modified graphene oxide nanocomposite coatings:

- nonisothermal cure kinetics study. *Progress in Organic Coatings*, 114, 233-243. <http://dx.doi.org/10.1016/j.porgcoat.2017.10.023>.
26. Zhou, T., Gu, M., Jin, Y., & Wang, J. (2005). Studying on the curing kinetics of a DGEBA/EMI-2, 4/nano-sized carborundum system with two curing kinetic methods. *Polymer*, 46(16), 6174-6181. <http://dx.doi.org/10.1016/j.polymer.2005.03.114>.
 27. Li, L., Zeng, Z., Zou, H., & Liang, M. (2015). Curing characteristics of an epoxy resin in the presence of functional graphite oxide with amine-rich surface. *Thermochimica Acta*, 614, 76-84. <http://dx.doi.org/10.1016/j.tca.2015.06.006>.
 28. Barros, J. J. P., Silva, I. D. S., Jaques, N. G., Fook, M. V. L., & Wellen, R. M. R. (2020). Influence of PCL on the epoxy workability, insights from thermal and spectroscopic analyses. *Polymer Testing*, 89, 106679. <http://dx.doi.org/10.1016/j.polymeresting.2020.106679>.
 29. Nakano, T., Ikawa, N., & Ozimek, L. (2003). Chemical composition of chicken eggshell and shell membranes. *Poultry Science*, 82(3), 510-514. <http://dx.doi.org/10.1093/ps/82.3.510>. PMID:12705414.
 30. Blaine, R. L., & Kissinger, H. E. (2012). Homer Kissinger and the Kissinger equation. *Thermochimica Acta*, 540, 1-6. <http://dx.doi.org/10.1016/j.tca.2012.04.008>.
 31. Criado, J. M., Sánchez-Jiménez, P. E., & Pérez-Maqueda, L. A. (2008). Critical study of the isoconversional methods of kinetic analysis. *Journal of Thermal Analysis and Calorimetry*, 92(1), 199-203. <http://dx.doi.org/10.1007/s10973-007-8763-7>.
 32. Šimon, P. (2004). Isoconversional methods. *Journal of Thermal Analysis and Calorimetry*, 76(1), 123-132. <http://dx.doi.org/10.1023/B:JTAN.0000027811.80036.6c>.
 33. Vyazovkin, S., & Sbirrazzuoli, N. (2006). Isoconversional kinetic analysis of thermally stimulated processes in polymers. *Macromolecular Rapid Communications*, 27(18), 1515-1532. <http://dx.doi.org/10.1002/marc.200600404>.
 34. Wu, F., Zhou, X., & Yu, X. (2018). Reaction mechanism, cure behavior and properties of a multifunctional epoxy resin, TGDDM, with latent curing agent dicyandiamide. *RSC Advances*, 8(15), 8248-8258. <http://dx.doi.org/10.1039/C7RA13233F>. PMID:35542009.
 35. Kamran-Pirzaman, A., Rostamian, Y., & Babatabar, S. (2020). Surface improvement effect of silica nanoparticles on epoxy nanocomposites mechanical and physical properties, and curing kinetic. *Journal of Polymer Research*, 27(1), 13. <http://dx.doi.org/10.1007/s10965-019-1918-y>.
 36. Achilias, D. S., Karabela, M. M., Varkopoulou, E. A., & Sideridou, I. D. (2012). Cure kinetics study of two epoxy systems with Fourier Transform Infrared Spectroscopy (FTIR) and Differential Scanning Calorimetry (DSC). *Journal of Macromolecular Science, Part A*, 49(8), 630-638. <http://dx.doi.org/10.1080/10601325.2012.696995>.
 37. Li, C., Bu, Z., Sun, J., Fan, H., Wan, J., & Li, B. (2013). New insights into high-ortho phenolic novolac: elucidating dependence between molecular structure, curing kinetics and thermal stability. *Thermochimica Acta*, 557, 77-86. <http://dx.doi.org/10.1016/j.tca.2013.01.004>.
 38. Roudsari, G. M., Mohanty, A. K., & Misra, M. (2014). Study of the curing kinetics of epoxy resins with biobased hardener and epoxidized soybean oil. *ACS Sustainable Chemistry & Engineering*, 2(9), 2111-2116. <http://dx.doi.org/10.1021/sc500176z>.
 39. Erdoğan, B., Seyhan, A. T., Ocak, Y., Tanoğlu, M., Balköse, D., & Ülkü, S. (2008). Cure kinetics of epoxy resin-natural zeolite composites. *Journal of Thermal Analysis and Calorimetry*, 94(3), 743-747. <http://dx.doi.org/10.1007/s10973-008-9366-7>.
 40. Paramarta, A., & Webster, D. C. (2017). Curing kinetics of bio-based epoxy-anhydride thermosets with zinc catalyst. *Journal of Thermal Analysis and Calorimetry*, 130(3), 2133-2144. <http://dx.doi.org/10.1007/s10973-017-6704-7>.
 41. Montserrat, S., Flaqué, C., Pagès, P., & Málek, J. (1995). Effect of the crosslinking degree on curing kinetics of an epoxy-anhydride system. *Journal of Applied Polymer Science*, 56(11), 1413-1421. <http://dx.doi.org/10.1002/app.1995.070561104>.
 42. Sun, G., Sun, H., Liu, Y., Zhao, B., Zhu, N., & Hu, K. (2007). Comparative study on the curing kinetics and mechanism of a lignin-based-epoxy/anhydride resin system. *Polymer*, 48(1), 330-337. <http://dx.doi.org/10.1016/j.polymer.2006.10.047>.

Received: Dec. 09, 2021

Revised: July 16, 2022

Accepted: Aug. 01, 2022

Supplementary Material

Supplementary material accompanies this paper.

Table S1. Curing parameters computed from DSC scans.

Figure S1. DSC scans for the investigated compounds at indicated heating rates. Effect of DEH 35 and eggshell membrane content.

Figure S2. Degree of conversion for S_5 and M_{10} at indicated heating rates.

Figure S3. Curing rate (min⁻¹) for S_5 and M_{10} at indicated heating rates.

Figure S4. Discrepancy between theoretical and experimental α using the Kissinger model at indicated heating rates. (a) S_5 ; and (b) M_{10} .

Figure S5. Discrepancy between theoretical and experimental α for Friedman isoconversional model at indicated heating rates. (a) S_5 ; and (b) M_{10} .

Figure S6. Discrepancy between theoretical and experimental α computed using the autocatalytic Friedman model. (a) S_5 ; and (b) M_{10} .

Figure S7. Discrepancy between theoretical and experimental α estimated using Málek model (a) S_5 ; and (b) M_{10} .

Figure S8. Discrepancy between theoretical and experimental α at 5 °C/min. Applied models indicated. (a) S_5 ; and (b) M_{10} .

Figure S9. Kissinger linear regression $\ln\left(\beta / T_p^2\right)$ versus $1000 / T_p$ for S_5 and M_{10} compounds.

Figure S10. Comparison between experimental and theoretical $d\alpha / dt$ estimated using Kissinger model at indicated rates. (a) S_5 ; and (b) M_{10} .

Figure S11. Friedman isoconversional linear regression $\ln(d\alpha / dt)$ versus $1000 / T_p$ for S_5 and M_{10} compounds.

Figure S12. Comparison between experimental and theoretical $d\alpha / dt$ estimated using Friedman isoconversional model at indicated rates. (a) S_5 ; and (b) M_{10} .

Figure S13. Comparison between experimental and theoretical $d\alpha / dt$ estimated using Friedman model based model at indicated rates. (a) S_5 ; and (b) M_{10} .

Figure S14. Málek functions $y(\alpha) e Z(\alpha)$ for S_5 at indicated heating rates.

Figure S15. Málek functions $y(\alpha) e Z(\alpha)$ for M_{10} at indicated heating rates.

Figure S16. Comparison between experimental and theoretical $d\alpha / dt$ estimated using Málek model at indicated rates. (a) S_5 ; and (b) M_{10} .

This material is available as part of the online article from <https://doi.org/10.1590/0104-1428.20210088>